Official URL

DOI : https://doi.org/10.1109/ISIT.2018.8437727

EBP-GEXIT charts over the binary-input AWGN channel for generalized and doubly-generalized LDPC codes

Arti D. Yardi[†], Iryna Andriyanova[‡], and Charly Poulliat[†]
[†] IRIT/INP-ENSEEIHT, University of Toulouse, France
[‡] ETIS-UMR 8051 Lab, University of Paris-Seine (University of Cergy-Pontoise/ENSEA/CNRS), France

***Abstract*—This work proposes a tractable evaluation of the maximum *a posteriori* (MAP) threshold of sparse-graph ensembles, by using an approximation for the extended belief propagation generalized extrinsic information transfer (EBP-GEXIT) function, first proposed by Measson et al. The approximation allows to find a MAP threshold in such numerically involved cases as the binary-input additive white Gaussian noise (AWGN) channel, graph ensembles with general component codes and/or irregularities. The paper contains examples of estimations of the MAP thresholds in the case of irregular low-density parity-check (LDPC), generalized LDPC, and doubly generalized LDPC codes ensembles. Our estimations are confirmed by numerical simulations.**

I. Introduction

The maximum *a posteriori* (MAP) threshold of a given channel code ensemble is defined as the minimum value of the channel parameter for which the average conditional entropy of a transmitted codeword is bounded away from zero [1, Sec. 4.7]. The average is taken over all possible randomly chosen codes in the given code ensemble as the length of the code goes to infinity. For the capacity achieving code ensemble, its MAP threshold reaches the fundamental limit on the channel parameter given by Shannon's channel coding theorem. It is known that performing the MAP decoding over any binary memoryless channel (BMS) is in general computationally intractable and this makes finding the MAP threshold also a difficult problem [1]. Finding the MAP threshold is thus an important yet difficult problem in the field of channel coding theory.

Méasson et al. have proposed a method to find the MAP threshold of a given code ensemble [2], [3]. In this method, the MAP threshold is obtained by applying the Maxwell construction to the EBP-GEXIT chart of a given code ensemble [2]. For the binary erasure channel, when the close form expression for the density evolution equation is known, the EBP-GEXIT chart can be obtained analytically [1]. However for any other BMS channel, obtaining this EBP-GEXIT chart is in general difficult. In this case, Méasson et al. have proposed a numerical method to find the EBP-GEXIT chart, using which one can find an estimate of the MAP threshold [3, Sec. VIII].

In this paper, we consider the binary input additive white Gaussian noise (AWGN) channel for which we provide a simple numerical approximation method to obtain the EBP-GEXIT chart of the given code ensemble. We assume that the distribution of the messages exchanged during the belief propagation (BP) decoding is consistent Gaussian [4, Ch. 9]. Note that this Gaussian assumption was initially proposed by Chung et al. [5]. This Gaussian assumption simplifies the operations performed at the check and variable nodes and enables us to find the EBP-GEXIT chart in a computationally feasible manner. We next summarize the main contributions of this paper.

(1) We propose a simple numerical method to obtain the EBP-GEXIT chart of the given code ensemble that makes use of the above mentioned Gaussian assumption.
(2) We compare the EBP-GEXIT charts obtained by our method with the method given by Méasson's et al. [3, Sec. VIII]. We observe that the EBP-GEXIT charts obtained by both the methods with Gaussian approximation are the same (see Fig. 1).
(3) Finally, we obtain the EBP-GEXIT chart of several generalized LDPC and doubly generalized LDPC codes and estimate their MAP thresholds.

The paper is organized as follows. We first recall some preliminaries related to the EBP-GEXIT chart in Section II. In Section III, we provide a numerical method to find the EBP-GEXIT chart of a given code ensemble. In Section IV section, we provide EBP-GEXIT chart of several generalized and doubly generalized LDPC codes and estimate their MAP-threshold. Finally, we discuss some future directions and conclude in Section V.

II. Preliminaries and notations

Let $\lambda(x) = \sum_i \lambda_i x^{i-1}$ and $\rho(x) = \sum_i \rho_j x^{j-1}$ be the degree distribution pair of an LDPC code ensemble from the edge perspective and let $\Lambda(x)$ and $P(x)$ be the corresponding normalized degree distribution pair from the node perspective. For irregular LDPC codes, all constraint nodes correspond to single parity check codes and variable nodes correspond to repetition codes [4]. When some of the check nodes correspond to any other linear block code, the LDPC code is referred to as generalized LDPC (GLDPC) code and when both variable and check nodes correspond to any general linear block code, the code is referred to as doubly generalized LDPC (DGLDPC) code [4]. We assume that variable nodes are unpunctured and have degree greater or equal to 2.

In this paper, we consider the transmission over a binary input AWGN channel where coded bits are modulated according to a binary phase shift keying and the additive noise is of zero mean and variance σ^2, The family of AWGN channels parameterized by σ will be denoted by $\{\text{AWGN}(\sigma)\}_\sigma$. Let $\mathcal{X}$ and $\mathcal{Y}$ be the channel input alphabet and output alphabets respectively. For the given AWGN(σ), the distribution of log likelihood ratios $L := \log \frac{\mathbb{P}[Y=y|X=+1]}{\mathbb{P}[Y=y|X=-1]}$ under the condition $X = +1$ is referred to as L-density and is denoted by c_σ [3, Sec. II]. The entropy $H(c_\sigma)$ of AWGN(σ) is then defined as

$$H(c_\sigma) = \int_{-\infty}^{\infty} c_\sigma(z)\log_2(1+e^{-z})\mathrm{d}z. \tag{1}$$

It can be seen that $H(c_\sigma) \in [0, 1]$. If $H(c_\sigma) = h$, AWGN(σ) can be equivalently described by its entropy h. Since h and σ can be obtained from one another, we can parametrize the family of AWGN channel either by h or σ. In the remaining paper, we use c_σ and c_h to represent the same L-density if $H(c_\sigma) = h$ and the corresponding AWGN channel is represented either by AWGN(σ) or by AWGN(h) .

Let f_C and f_V be the functions corresponding to the operations performed at the check and variable nodes respectively while performing BP decoding. When the all-one codeword is transmitted, let $a^{BP,l}$ be the density of the message transmitted by any randomly chosen variable node to check node in the l-th iteration of BP decoding. For the first iteration, $a^{BP,0}$ is initialized to c_h. For $l \geq 1$, $a^{BP,l}$ can be obtained from $a^{BP,l-1}$ as follows

$$a^{BP,l} = c_h \star f_V(f_C(a^{BP,l-1})), \tag{2}$$

where the operator $\star$ is the convolution operator associated to the operations performed in one iteration of the BP decoding (for details refer [1, Sec. 4.1.4]). For an irregular LDPC code, $f_C(.) = \rho(.)$ and $f_V = \lambda(.)$ [1, Theorem 4.97]. For GLDPC codes and DGLDPC codes, the operations performed at check and variable node are more complex.

We now recall the definition the EBP-GEXIT chart [3, Sec. VII-A]. Let us first define a complete fixed-point family. The family of densities $\{a_x\}_x$ and $\{c_x\}_x$ parameterized by $x \in [0, 1]$ is called a complete fixed-point family if the following conditions are satisfied.

1) $c_x \in \{\text{AWGN}(h)\}_h$ for some $h \in [0, 1]$,
2) For any $x \in [0, 1]$ we have $a_x = c_x \star f_V(f_C(a_x))$, i.e., a_x is a fixed point density with respect to c_x,
3) $H(a_x) = x$,
4) $\{a_x\}_x$ and $\{c_x\}_x$ are smooth with respect to x.

The EBP-GEXIT function $g^{EBP}(x)$ for an LDPC code ensemble with degree distribution pair (λ, ρ) is then defined as [3, Sec. VII-A]

$$g^{EBP}(x) := \int_{-\infty}^{\infty} \Lambda(f_C(a_x))(z)l(c_x(z))\mathrm{d}z, \tag{3}$$

where $l(c_x(z))$ is defined as follows [3, Example 7]

$$l(c_x(z)) = \left(\int_{-\infty}^{\infty} \frac{e^{-\frac{(w-(2/\sigma^2))^2}{8/\sigma^2}}}{1+e^{w+z}}\mathrm{d}w\right) \Big/ \left(\int_{-\infty}^{\infty} \frac{e^{-\frac{(w-(2/\sigma^2))^2}{8/\sigma^2}}}{1+e^{w}}\mathrm{d}w\right). \tag{4}$$

The EBP-GEXIT chart is the curve obtained by plotting $g^{EBP}(x)$ versus c_x for all possible values of $x \in [0, 1]$.

III. EBP-GEXIT CHART OVER AWGN

In this section, we propose a simple numerical method to find the EBP-GEXIT chart of a given LDPC code ensemble. As explained in the previous section, in order to plot the EBP-GEXIT chart, we need to first find a fixed point density a for a given channel c_h, i.e., we need to find a pair of densities a and c_h that satisfy the following equation

$$a = c_h \star f_V(f_C(a))). \tag{5}$$

Note that the density a corresponds to a message transmitted by a variable node to a check node in the BP decoding. We assume that the distribution of a is a consistent normal distribution, i.e., for some real number m_a, distribution of a is normal with mean m_a and variance $2m_a$, denoted by $\mathcal{N}(m_a, 2m_a)$. This Gaussian assumption is proposed by Chung et al. [5] and also used for classical EXIT charts analysis [6]. We shall next explain how this Gaussian assumption simplifies the operations required to find EBP-GEXIT curve.

First, we explain how $c_h \star f_V(f_C(a)))$ in (5) can be efficiently approximated using a classical approximation by an EXIT-like monodimensional fixed point equation. For a given density $a = \mathcal{N}(m_a, 2m_a)$, consider the function $J(m_a)$ defined as follows

$$J(m_a) := 1 - \mathbb{E}_a\big[\log_2(1+e^{-y})\big], \tag{6}$$

where $\mathbb{E}_a$ denotes expectation with respect to a. Approximate values of the functions $J(.)$ and $J^{-1}(.)$ can be deduced from [6]. Further, the function $J(.)$ is a one-to-one function and this implies that the density a can be uniquely determined from it. Using EXIT based monodimensional representation, the fixed point equation (5) can be equivalently stated using some abuse of notations as follows

$$J(m_a) = c_h \circledast f_V\big[f_C\big(J(m_a)\big)\big], \tag{7}$$

where the operator $\circledast$ corresponds to the change of operation occurred due to change from density a to $J(m_a)$. For the irregular LDPC codes, the operations $f_C(.)$ and $f_V(.)$ can be simplified as follows [4]

$$f_C(J(m_a)) = \sum_j \rho_j\Big(1 - J\Big[(j-1)J^{-1}(1-J(m_a))\Big]\Big)$$
$$c_h \circledast f_V(f_C(m_a))) = \sum_i \lambda_i J\Big[(i-1)J^{-1}\big[f_C(m_a)\big] + \frac{2}{\sigma^2}\Big] \tag{8}$$

where $2/\sigma^2$ is the mean of the L-density c_h. Note that, (7) can now be efficiently computed using (8). For GLDPC and DLDPC codes, the functions $f_C(.)$ and $f_V(.)$ are evaluated point-wise by means of Monte Carlo simulations (details are given in [7] and [8]).

We now explain how the EBP-GEXIT function can be computed efficiently. To this end, we first need to derive $\Lambda(f_C(a))$ (see equation (3)) under our Gaussian assumption. Let b denotes the density of the messages coming from the check nodes. Suppose this density is consistent Gaussian with mean m_b. For a variable node of degree j, the density obtained by taking the convolution of the input density j times is the consistent Gaussian density of mean jm_b. Let us denote this density by b_j. The density $\Lambda(b)$ is thus the mixture of densities b_j given by

$$\Lambda(b)(z) = \sum_j \Lambda_j b_j(z), \tag{9}$$

where $b_j(z)$ is given by,

$$b_j(z) = \frac{1}{\sqrt{4\pi j m_b}} \exp\left(-\frac{z - jm_b}{4jm_b}\right). \tag{10}$$

Substituting (9) in (3) we get,

$$\begin{aligned} g^{EBP} &= \int_{-\infty}^{\infty} \Big[\sum_j \Lambda_j b_j(z)\Big] l(c_h(z))\mathrm{d}z, \\ &= \sum_j \Lambda_j \int_{-\infty}^{\infty} b_j(z) l(c_h(z))\mathrm{d}z, \qquad (11) \\ &= \sum_j \Lambda_j \mathbb{E}_{b_j}\Big[l(c_h(z))\Big]. \end{aligned}$$

Observe that $\mathbb{E}_{b_j}\big[l(c_h(z))\big]$ is now expectation over a Gaussian density b_j. This expectation can be efficiently computed using the Gauss-Hermit quadrature weights as follows [9]:

- For some integer d, let H_d be the Hermite polynomial of degree d and let $k_1, k_2, \dots, k_d$ be its roots.
- Let $z_i = \sqrt{4jm_b}k_i + jm_b$. Then an approximate value of $\mathbb{E}_{b_j}\big[l(c_h(z))\big]$ is given by

$$\mathbb{E}_{b_j}\big[l(c_h(z))\big] \approx \frac{1}{\sqrt{\pi}} \sum_{i=1}^{d} \frac{2^{d-1} d! \sqrt{\pi}}{d^2 [H_{d-1}(k_i)]^2} l(c_h(z_i)), \tag{12}$$

  where $l(c_h(z))$ is defined in (4) and can be computed using numerical integration.

To summarize, using the Gaussian assumption, the fixed point density in (5) is now represented by fixed point equation (7) since both $J(m_a)$ and h take values in the interval $[0, 1]$. Further, the Gaussian assumption provides an efficient computation of the EBP-GEXIT function via Gauss-Hermit quadrature weights. Using these simplifications, we now propose an algorithm to find the EBP-GEXIT chart of a given LDPC code ensemble in Algorithm 1. The basic idea of the proposed algorithm consists of finding all possible a and c_h pairs that satisfy (5). All such pairs are found efficiently via grid search by varying $J(m_a)$ and h in the range $[0, 1]$. It is important to mention that the consistent Gaussian assumption makes this a grid search and evaluation of EBP-GEXIT function computationally feasible.

Algorithm 1 EBP-GEXIT chart over AWGN

1) **Choose** $h \in [0, 1]$ and let c_h be the L-density corresponding to AWGN(h).
2) **Find** $\mathcal{S}_h := \big\{J(m_a) : \text{such that } J(m_a) \text{ satisfies (7)}\big\}$, by varying $J(m_a)$ in the range $[0, 1]$. (The calculations are performed using (8)).
3) The set of densities a corresponding to $\mathcal{S}_h$ provide a set of points on the EBP-GEXIT curve. For each a obtained in step (2), **compute** g^{EBP} using (11), (12).
4) **Plot** all possible values g^{EBP} obtained in step (3) versus the chosen h.
5) **Repeat** the process for various values of $h \in [0, 1]$.

Remark 1. *On contrary to the definition of complete fixed-point family, a and c_h pairs obtained using Algorithm 1 are not parameterized by some $x \in [0, 1]$, since we find these pairs exhaustively. However it can be easily verified that $H(a) = x$ for some $x \in [0, 1]$ and the set of a and c_h obtained do form a complete fixed-point family.* □

IV. Obtained Results

In this section, we first compare the EBP-GEXIT chart obtained using the proposed method with the method of [3] for various irregular LDPC codes. We then obtain EBP-GEXIT chart for various GLDPC and DGLDPC codes using the proposed algorithm and estimate their corresponding BP and MAP thresholds. An estimate of the MAP threshold is obtained by applying Maxwell's construction to each EBP-GEXIT chart (the details about Maxwell's construction can be found in [1, Sec. 3.20]).

A. EBP-GEXIT chart for irregular LDPC codes

Méasson et al. have proposed a numerical method to find the EBP-GEXIT chart for a given LDPC code ensemble [3, Sec. VIII]. In Figures 1 to 4 we plot the EBP-GEXIT charts obtained by Méasson's method and our method for various regular and irregular LDPC codes. For plotting the EBP-GEXIT chart using Méasson's method also we consider the Gaussian assumption explained in first paragraph of this section. It can be seen that the EBP-GEXIT charts obtained by both the methods are the same.

B. EBP-GEXIT chart for GLDPC and DGLDPC codes

In this section, several examples of GLDPC and DGLDPC codes are considered and their BP and MAP thresholds are estimated. To illustrate our approach, let us estimate BP and MAP thresholds of the following code examples:

- C_1: $(2, 7)$-regular ensemble of design rate $1/7$ based on the Hamming$(7, 4)$ component code
- C_2: $(2, 15)$-regular ensemble of design rate $7/15$ based on the Hamming$(15, 11)$ component code designed in [7]

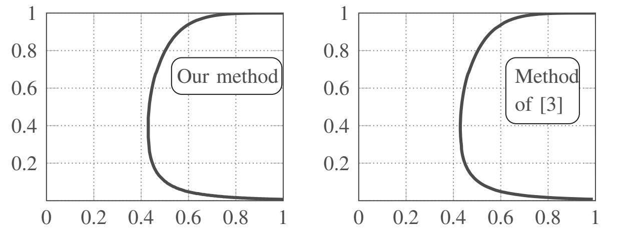

Fig. 1. The EBP-GEXIT chart of LDPC code ensemble with $\lambda(x) = x^2$ and $\rho(x) = x^5$ is illustrated for our method (left side) and for the method of [3] (right side).

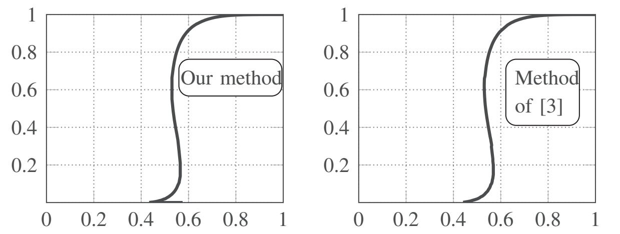

Fig. 2. The EBP-GEXIT chart of LDPC code ensemble with $\lambda(x) = 2/5x + 3/5x^5$ and $\rho(x) = x^5$ is illustrated for our method (left side) and for the method of [3] (right side).

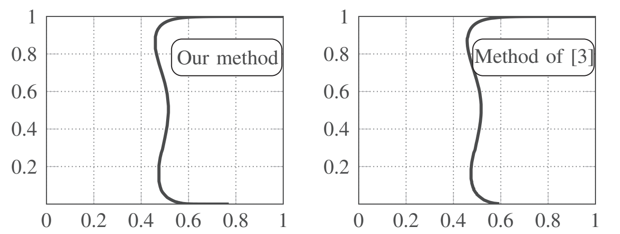

Fig. 3. The EBP-GEXIT chart of LDPC code ensemble with $\lambda(x) = \frac{3x+6x^2+11x^{17}}{20}$ and $\rho(x) = x^9$ is illustrated for our method (left side) and for the method of [3] (right side).

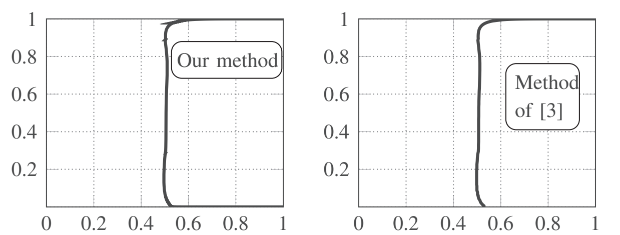

Fig. 4. The EBP-GEXIT chart of LDPC code ensemble with $\lambda(x) = 0.17120x + 0.21053x^2 + 0.00273x^3 + 0.00009x^6 + 0.15269x^7 + 0.09227x^8 + 0.02802x^9 + 0.01206x^{14} + 0.07212x^{29} + 0.2583x^{49}$ and $\rho(x) = 0.33620x^8 + 0.08883x^9 + 0.57497x^{10}$ is illustrated for our method (left side) and for the method of [3] (right side). This is a capacity achieving ensemble [10].

- C_3: DGLDPC ensemble of rate $3/4$ from [8]
- C_4: DGLDPC ensemble of rate $7/15$ from [11]
- C_5: 3-regular GLDPC ensemble of rate $1/2$ based on a TLDPC component code [12]
- C_6: irregular GLDPC ensemble of rate $1/2$ from with a TLDPC component code [12]

The ensembles C_3 and C_4 have the following structure. Let the generator matrices G_1, G_2 and G_3 be $G_1 = \begin{bmatrix} 1 & 1 & 1 & 1 & 0 & 0 \\ 0 & 0 & 1 & 1 & 1 & 1 \end{bmatrix}, G_2 = \begin{bmatrix} 1 & 0 & 0 & 1 & 1 & 0 \\ 0 & 1 & 0 & 0 & 1 & 1 \\ 0 & 0 & 1 & 1 & 0 & 1 \end{bmatrix}, G_3 = \begin{bmatrix} 1 & 1 & 1 & 0 & 0 & 0 \\ 0 & 1 & 1 & 1 & 0 & 0 \\ 0 & 0 & 1 & 1 & 1 & 0 \\ 0 & 0 & 0 & 1 & 1 & 1 \end{bmatrix}$. Then both C_3 and C_4, have variable nodes of constant degree 6. The variable nodes for C_3 correspond to repetition codes of length 6 (69% of all nodes), linear codes defined by G_2 (1%), linear codes defined G_3 (22%) and single parity check codes of length 6 denoted by SPC(6) (8%). On the check node side, nodes correspond to SPC(12). The variable nodes for C_4 correspond to repetition codes of length 6 (42.5% of all nodes), codes defined by G_1 (7.5%), codes defined by G_3 (7.5%), and SPC(6) (42.5%). Component codes for C_4 are Hamming $(15, 11)$ codes. Codes C_5 and C_6 are GLDPC ensembles belonging to the class of TLDPC codes of type B, designed in [12]. C_5 is a 3-regular code, while C_6 has the following degree distribution of variable nodes $\lambda(x) = 0.5x + 0.182x^2 + 0.069x^{12} + 0.249x^{13}$ which has been optimized in [12] to improve the BP threshold.

EBP-GEXIT charts of codes from C_1 to C_6 are given in Fig. 5, 6 and 7. Based on these curves, BP and MAP thresholds of the ensembles have been estimated (dashed lines in figures), and the results are reported to Table I.

Finally, in order to show the validity of our estimations, let us compare them with numerical simulations. Fig. 8 shows the bit error rates over the AWGN for spatially-coupled versions of codes from C_5 with a spatial coupling parameter w. It is known that [13], [14], the spatially-couple ensemble has a BP threshold that approaches the MAP threshold with w (and it equals to the (non-coupled) BP threshold for $w = 0$). Referring to Table I, the BP threshold for C_5 is 1.4264 dB ($h = 0.4035$) and the MAP threshold – 0.5548 dB ($h = 0.4719$). Referring to Fig.8, the thresholds of spatially-coupled ensembles with $w = 1$ and $w = 3$ are around $0.9 - 0.95$ dB, this is consistent with Table I.

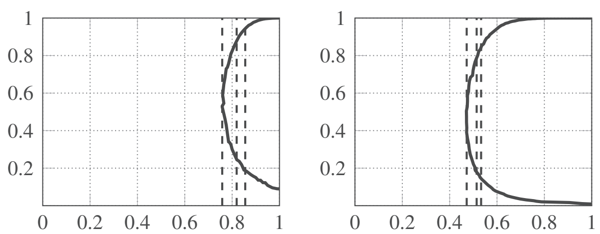

Fig. 5. EBP-GEXIT chart for C_1 (left) and for C_2 (right).

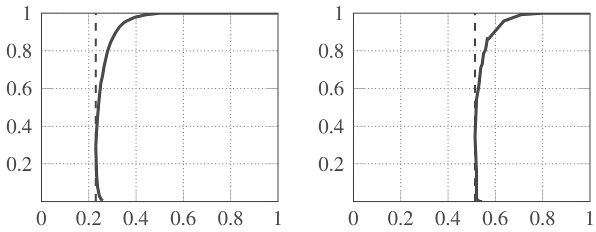

Fig. 6. EBP-GEXIT charts for C_3 (left) and C_4 (right).

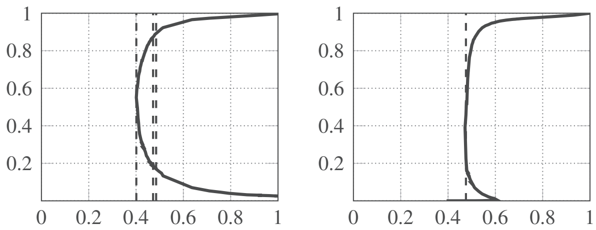

Fig. 7. EBP-GEXIT charts for C_5 (left) and C_6 (right).

LDPC Ensemble	BP (literature)	Our BP estimate	Our MAP Estimate	Upper Bound on MAP Threshold [3]
GLDPC C_1 (Hamm(7))	0.756 [15]	0.7582	0.8191	0.8554
GLDPC C_2 (Hamm(15))	0.478 (0.75dB) [7]	0.4719	0.5140	0.5328
DGLDPC C_3	0.23 (1.9dB) [8]	0.2296	0.2296	0.2296
DGLDPC C_4	0.514 (0.3dB) [11]	0.514	0.514	0.514
TLDPC C_5	0.4035	0.4011	0.4719	0.4849
TLDPC C_6	0.478 (0.45dB)	0.4756	0.4756	0.4756

TABLE I
COMPARISON OF BP AND MAP THRESHOLD VALUES (IN h) FOR GLDPC AND DGLDPC EXAMPLES

V. CONCLUSIONS AND FUTURE WORK

We propose a tractable and fast MAP threshold evaluation for graph ensembles, based on the Gaussian approximation. It works well for cases where using the method from [3] is too involved (e.g., over the AWGN channel), and numerical results are tight. Our method can be extended to ensembles with punctured bits and to ensembles having bits of degree 1. This will make object of our future work.

ACKNOWLEDGMENTS

This work is supported by ANR-11-LABEX-0040-CIMI within the program ANR-11-IDEX-0002-02 of Centre International de Mathématiques et Informatique de Toulouse, France.

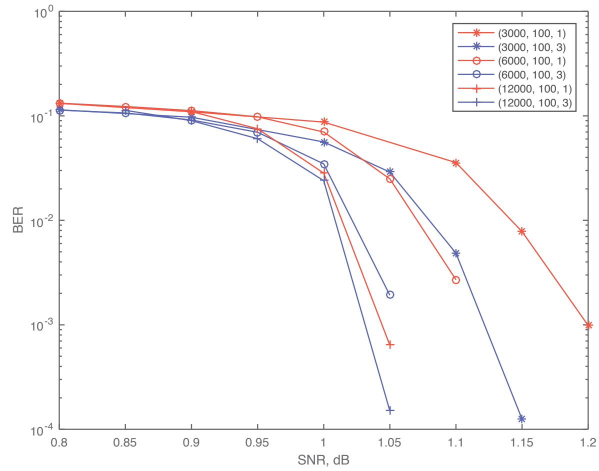

Fig. 8. Bit error rate vs. SNR (dB) for (n, L, w) spatially-coupled codes from the ensemble C_5 with total code length nL (n=3000,6000,12000), coupling parameter w (w=1,3) and the two-side termination.

REFERENCES

[1] T. Richardson and R. Urbanke, *Modern Coding Theory*. Cambridge University Press, 2008.
[2] C. Méasson, A. Montanari, and R. Urbanke, "Maxwell construction: The hidden bridge between iterative and maximum a posteriori decoding," *IEEE Transactions on Information Theory*, vol. 54, no. 12, pp. 5277–5307, December 2008.
[3] C. Méasson, A. Montanari, T. Richardson, and R. Urbanke, "The generalized area theorem and some of its consequences," *IEEE Trans. on Info. Theory*, vol. 55, no. 11, pp. 4793–4821, Nov. 2009.
[4] W. Ryan and S. Lin, *Channel codes: classical and modern*. Cambridge University Press, 2009.
[5] S. Chung, T. Richardson, and R. Urbanke, "Analysis of sum-product decoding of LDPC codes using a gaussian approximation," *IEEE Trans. on Info. Theory*, vol. 47, no. 2, pp. 657–670, Feb. 2001.
[6] A. Ashikmin, G. Kramer, and S. ten Brink, "Extrinsic information transfer functions: Model and erasure channel properties," *IEEE Trans. on Info. Theory*, vol. 50, no. 11, pp. 2657–2673, Nov. 2004.
[7] G. Liva, W. Ryan, and M. Chiani, "Quasi-cyclic generalized LDPC codes with low error floors," *IEEE Transactions on Communications*, vol. 56, no. 1, pp. 49–57, January 2008.
[8] Y. Wang and M. Fossorier, "Doubly generalized LDPC codes," in *Proceedings of IEEE International Symposium on Information Theory*, Seattle, WA, USA, July 2006, pp. 669–673.
[9] M. Abramowitz and I. Stegun, *Handbook of Mathematical Functions*. New York, USA: Dover, 1970.
[10] T. Richardson, M. Shokrollahi, and R. Urbanke, "Design of capacity-approaching irregular low-density parity-check codes," *IEEE Trans. on Information Theory*, vol. 47, no. 2, pp. 619–637, Feb. 2001.
[11] Y. Wang and M. Fossorier, "EXIT chart analysis for doubly generalized LDPC codes," in *Proceedings of IEEE Globecomm*, San Francisco, California, USA, November 2006, pp. 1–6.
[12] I. Andriyanova, J.-P. Tillich, and J.-C. Carlach, "Asymptotically good codes with high iterative decoding performances," in *Proceedings of IEEE ISIT*, Adelaide, Australia, September 2005, pp. 850–854.
[13] S. Kudekar, T. Richardson, and R. Urbanke, "Threshold saturation via spatial coupling: Why convolutional LDPC ensembles perform so well over the BEC," *IEEE Transactions on Information Theory*, vol. 57, no. 2, pp. 803–834, Feb. 2011.
[14] A. Giurgiu, N. Macris, and R. Urbanke, "Spatial coupling as a proof technique and three applications," *IEEE Transactions on Information Theory*, vol. 62, no. 10, pp. 5281–5295, 2016.
[15] M. Lentmaier and G. Fettweis, "On the thresholds of generalized LDPC convolutional codes based on protographs," in *Proceedings of IEEE ISIT*, Austin, Texas, USA, June 2010, pp. 709–713.